Results in Applied Mathematics 21 (2024) 100415

Contents lists available at ScienceDirect

Results in Applied Mathematics

journal homepage: www.elsevier.com/locate/results-in-applied-mathematics

Wavelets collocation method for singularly perturbed differential–difference equations arising in control system

Shahid Ahmed [a], Shah Jahan [a,*], Khursheed J. Ansari [b,*], Kamal Shah [c], Thabet Abdeljawad [c]

[a] Department of Mathematics, Central University of Haryana, Mahendergarh 123031, India
[b] Department of Mathematics, College of Science, King Khalid University, Abha, 61413, Saudi Arabia
[c] Department of Mathematics and Sciences, Prince Sultan University, P.O. Box 66833, Riyadh 11586, Saudi Arabia

ARTICLE INFO

MSC:
65L10
65L11
65T60
42C40

Keywords:
Collocation point
Control system
Haar wavelet
Multiresolution analysis
Singularly perturbed differential–difference equations

ABSTRACT

In this paper, we present a wavelet collocation method for efficiently solving singularly perturbed differential–difference equations (SPDDEs) and one-parameter singularly perturbed differential equations (SPDEs) taking into account the singular perturbations inherent in control systems. These equations represent a class of mathematical models that exhibit a combination of differential and difference equations, making their analysis and solution challenging. The terms that include negative and positive shifts were approximated using Taylor series expansion. The main aim of this technique is to convert the problems by using operational matrices of integration of Haar wavelets into a system of algebraic equations that can be solved using Newton's method. The adaptability and multi-resolution properties of wavelet functions offer the ability to capture system behavior across various scales, effectively handling singular perturbations present in the equations. Numerical experiments were conducted to showcase the effectiveness and accuracy of the wavelet collocation method, demonstrating its potential as a reliable tool for analyzing and solving SPDDEs in control system.

1. Introduction

A SPDDEs is a type of differential equation that exhibits a specific characteristic. In these equations, the highest-order derivative terms are multiplied by a small positive parameter [1]. Additionally, singularly perturbed differential–difference equations involve the presence of at least one term containing a delay or advance in time, or even a combination of both Delay and advance have been referred to as negative shift and positive shift in recent literature. Singularly perturbed boundary layer problems have been the focus of numerous researchers over the past two decades owing to their relevance throughout the modeling of many real-life phenomena in engineering and science [2–11]. Control systems play a crucial role in a wide range of applications, from industrial processes to robotics and aerospace systems. The accurate modeling and analysis of control systems often involve addressing the challenges posed by SPDDEs. These equations arise due to the combined presence of differential and difference equations, reflecting the continuous and discrete dynamics inherent in control systems. Whenever a physical system is mathematically modeled such as In control theory, small temporal parasitic components, such as moments of inertia, capacitances, and resistances, can significantly impact the behavior and performance of control systems. These parasitic components arise due to physical characteristics and limitations of the system being controlled and can introduce additional dynamics and delays [12,13]. The system order is decreased when these tiny constants

* Corresponding authors.
E-mail addresses: chowdharyshahjahan@gmail.com (S. Jahan), ansari.jkhursheed@gmail.com (K.J. Ansari).

https://doi.org/10.1016/j.rinam.2023.100415
Received 24 September 2023; Received in revised form 15 November 2023; Accepted 20 November 2023
Available online 22 December 2023
2590-0374/© 2023 The Author(s). Published by Elsevier B.V. This is an open access article under the CC BY license (http://creativecommons.org/licenses/by/4.0/).

are suppressed, these systems are known as singular perturbation systems and they are classified as singularly perturbed delay differential equations when they account for both the physical system in past and present states [5,6,9,12,14]. In these types of issues, perturbations operate across a relatively small area, causing the dependent variable to change very quickly because the small parameter multiplies the largest derivative. These narrow regions usually border the edges or a point inside the domain of interest. Therefore, these kinds of problems exhibit boundary and interior layers where the solution changes rapidly [15]. SPDDEs play a key role in the mathematical modeling of a wide range of real-world events in neural variability [10], bioscience and control theory [13], in determining the anticipated time for random synaptic action potential production in nerve cells, study on the human pupil light reflex [16], mathematical biology [13], diverse physiological process models [12], and disease controllability [7].

In the current article, we have solved two types of SPDEs. Firstly we consider one parameter singularly perturbed boundary value problem as:

$$-\epsilon\frac{d^2y}{d\zeta^2}+q(\zeta)y(\zeta)=S(\zeta),\quad \zeta\in(0,1), \tag{1}$$

defined on $[0,1]$ and satisfy the following BCs

$$y(0)=\alpha,\quad y(1)=\beta,$$

where $S(\zeta)$, $q(\zeta)$ are smooth functions and ϵ is a small parameter. Secondly, we consider SPDDEs with delay and shift as follows:

$$\epsilon^2\frac{d^2y}{d\zeta^2}+b(\zeta)y(\zeta-\delta)+c(\zeta)y(\zeta)+d(\zeta)y(\zeta+\mu)=R(\zeta),\quad \zeta\in(0,1), \tag{2}$$

subject to boundary conditions(BCs)

$$y(\zeta)=g(\zeta)\,,\quad -\delta\le\zeta\le 0$$

and

$$y(\zeta)=g_1(\zeta)\,,\quad 1\le\zeta\le 1+\mu,$$

where $b(\zeta)$, $c(\zeta)$, $d(\zeta)$, $g(\zeta)$, $g_1(\zeta)$ and $R(\zeta)$ are sufficiently smooth functions the perturbation parameter is denoted by ϵ that is $0<\epsilon\le 1$, the delay and shifting parameters are δ and μ respectively which depends upon ϵ. Applications of the class of perturbed problems (1) and (2) found in science and engineering such as quantum mechanics [12] fluid mechanics, reaction–diffusion process [17] chemical-reactor theory [18] optimal control [19] and geophysics [5,10,15]. Numerous techniques for these models have been given and examined from a numerical perspective. The vast majority of numerical techniques currently in use are based on finite element techniques [20]. A survey of several asymptotic and numerical techniques for solving SPDDEs is found in [16]. Various other methods such as septic B-spline method for boundary value problem [21], exponential fitted finite difference method [22]. Fourth-order stable central difference method [16], exponentially B-spline collocation method [23], Non-polynomial sextic spline method [24] and numerical analysis of boundary value problems for SPDDEs with small shifts of mixed type with rapid oscillation are discussed in [24,25]. It is notably challenging to establish oscillation-free solutions on a uniform grid for the SPDDEs because of the co-existence of singular perturbation (ϵ) and shift arguments. Upon careful examination of the findings, it has been observed that conventional numerical approaches, such as finite difference, finite element, and volume methods implemented on uniform grids, face limitations in providing satisfactory numerical solutions as the perturbation parameter ϵ approaches zero. These methods often require an excessively large number of mesh points or the implementation of an adaptive layer mesh in order to obtain accurate results. The truncation error grows unboundedly as the mesh size decreases [16]. This demonstrates the computational inefficiency and high expense of the traditional numerical methods. Increasing the number of mesh points may lead to ill-conditioned systems of algebraic equations because of this shortcoming researchers are motivated to create reliable numerical techniques for SPDDEs. Wavelet-based methods achieved great success in solving differential equations numerically due to their computational simplicity straightforward methodology and speedy convergence [18,26–29]. The most frequently used wavelets for solving differential equations include Legendre wavelets [28] Bernoulli wavelets and Gegenbaur wavelets [29], Taylor wavelets, Fibonacci wavelets [30] and Haar wavelets [31]. The Haar wavelet possesses a piecewise constant shape, characterized by its ability to efficiently capture discontinuities in signals or functions. Its simplicity allows for straightforward implementation and computation, reducing the computational cost compared to more complex wavelet functions [26]. A. Raza et al. [32] used Haar wavelet for the solution of the neutral delay differential equation and also they solved [17] SPDDEs and convection delayed dominated diffusion equation. Lipik [31], has established the Haar wavelet method to solve ordinary and partial differential equations. Hussain et al. [33] discussed the solution of proportional-delay Riccati differential equations using Haar Wavelet. Imran Aziz [34] used Haar wavelet to solve the second-order boundary value problem. Sapna et al. [27] solved two parameter perturbed problems using the wavelet collocation method. The advantages of Haar wavelets over other wavelet families and their appealing features deeply motivate us to solved SPDDEs and one parameter singularly perturbed problem by the proposed method. The aim of this study is to present the Haar wavelet collocation approach to solve SPDEs. The wavelets collocation method is a reliable and effective way to solve SPDDEs that come up in control system applications. It is a useful tool for analyzing and developing control systems in many different areas because it can handle localized features and change to solution characteristics. The article is organized as follows, in Section 2 some properties of the continuous problem is given and in Section 3 a brief introduction of the wavelet and multiresolution analysis is discussed. The development of the Haar wavelet collocation approach for the solution of SPDDEs is covered in Section 4. Section 5, yields the Convergences and error analysis. In Section 6 we present some numerical results to illustrate the efficiency and accuracy of the proposed numerical method, and in Section 7 conclusion is drawn.

2. Some properties of the continuous problem

In this section, we establish the existence and uniqueness of the solution of SPDEs by the assumption that the data are Holder continuous and imposing appropriate compatibility conditions at the boundary points.

Lemma 2.1. *By imposing the compatibility conditions $\zeta = 0$ at boundary condition $y(0) = \alpha$, $\zeta = 1$ at $y(1) = \beta$ and*

$$-\epsilon \frac{d^2y(0)}{d\zeta^2} + q(0)y(0) = S(0), \quad -\epsilon \frac{d^2y(1)}{d\zeta^2} + q(1)y(1) = S(1)$$

so that the data matches at the boundary points. Let $S(\zeta)$, $q(\zeta)$ be continuous on domain. Then the problem SPDEs has unique solution $y(\zeta)$.

It is important to note that when $\epsilon = 0$, the problem reduces to a simpler form without the perturbation term. To show the bounds of the solutions $y(\zeta)$ of given problems, we assume without loss of generality the initial condition to be zero. Since $y_0(\zeta)$ is sufficiently smooth and using the property of norm, we prove the following lemma.

Lemma 2.2. ***Continuous Maximum Principle:*** *Let y be a sufficiently smooth function defined on D which satisfies $y(\zeta) \geq 0, \forall \zeta \in \partial D$. Then, if $Ly(\zeta) > 0, \forall \zeta \in D$, it implies that $y(\zeta) \geq 0, \forall \zeta \in \bar{D}$, where $Ly = -\epsilon y_{\zeta\zeta} + q(\zeta)y_{\zeta} - S(\zeta)$.*

Proof. The proof can be seen in [20] □

This maximum principle leads immediately to the following uniform stability result.(see the proof in Bobisud [35])

Theorem 2.1. *Let u be the solution of the problem (1) with boundary conditions exists, is unique and satisfies $\|y\| \leq \theta^{-1}\|S\| + C(\|\alpha\| + \|\beta\|)$ where $C \geq 1$ is a positive constant.*

Proof. See proof [20] □

3. Wavelets and multiresolution analysis

Wavelets are characterized as oscillations that have limited durations, starting from zero, reaching a maximum amplitude, and then returning to zero. They can be found in various waveforms, each with its unique properties. Among the different wavelet families, the Haar wavelet holds a significant position. It was first introduced by Alfred Haar in 1910 and stands as the oldest, simplest, and most fundamental wavelet family in terms of orthonormality. The Haar wavelet family for $\zeta \in [0, 1]$ can be defined as.

$$h_i(\zeta) = \begin{cases} 1 & \text{for} \quad \alpha \leq \zeta < \beta \\ -1 & \text{for} \quad \beta \leq \zeta < \gamma \\ 0 & \text{otherwise.} \end{cases} \tag{3}$$

$$\alpha = \frac{k}{m}, \quad \beta = \frac{k + 0.5}{m}, \quad \gamma = \frac{k + 1}{m}.$$

Here m, $k \in \mathbb{Z}$ as $m = 2^j, j = 0, 1, \ldots, J$ and J is the maximal level of resolution and the translation parameter is k where $k = 0, 1, \ldots, m - 1$. The index of h_i in (3) is given by $i = m + k + 1$. For $m = 1, k = 0$, we have $i = 2$, is the minimal values and $N = 2m = 2^{j+1}$ is the maximal value. For $i = 1$ the scaling function as

$$h_i(\zeta) = \begin{cases} 1 & \text{for} \quad 0 \leq \zeta < 1 \\ 0 & \text{otherwise.} \end{cases}$$

We refer to [26,27,33,34] for further information on Haar wavelets and their applications. Any square integrable function $f \in L^2[0, 1]$ can be expanded via Haar wavelets series:

$$f(\zeta) = a_0h_0(\zeta) + a_1h_1(\zeta) + a_2h_2(\zeta) + \cdots = \sum_{i=0}^{\infty} a_ih_i(\zeta),$$

where a_i, $i = 0, 1, 2, \ldots$ are the Haar coefficients given by

$$a_i = \langle f, h_i \rangle = \int_0^1 f(\zeta)h_i(\zeta)\, d\zeta.$$

The preceding series terminates finitely if $f(\zeta)$ is piecewise constant throughout each subinterval or is piecewise constant. Consequently, the discrete form can be expressed in matrix form as:

$$F \approx \sum_{i=0}^{m-1} a_ih_i(\zeta) = A_m^T H_m,$$

$A_m^T = [a_0, a_1, \dots, a_{m-1}]$ are the row vectors of dimension m and H_m of order $m = 2^M$ is the Haar wavelet matrix given in [26].

$$H_m = \begin{pmatrix} h_0 \\ h_1 \\ h_2 \\ h_3 \\ \vdots \\ h_{m-1} \end{pmatrix} = \begin{pmatrix} h_{0,0} & h_{0,1} & h_{0,2} & h_{0,3} & \dots & h_{0,m-1} \\ h_{1,0} & h_{1,1} & h_{1,2} & h_{1,3} & \dots & h_{1,m-1} \\ h_{2,0} & h_{2,1} & h_{2,2} & h_{2,3} & \dots & h_{2,m-1} \\ h_{3,0} & h_{3,1} & h_{3,2} & h_{3,3} & \dots & h_{3,m-1} \\ \vdots & \vdots & \vdots & \vdots & & \\ h_{m-1,0} & h_{m-1,1} & h_{m-1,2} & h_{m-1,3} & \dots & h_{m-1,m-1} \end{pmatrix}$$

The collocation points are defined as:

$$\zeta_l = \frac{l - 0.5}{2M} \quad l = 1, 2, \dots, 2M. \tag{4}$$

The Haar matrix of order 8 i.e., $j = 2 \Rightarrow N = 8$ is given below [26]

$$H_8 = \begin{pmatrix} 1 & 1 & 1 & 1 & 1 & 1 & 1 & 1 \\ 1 & 1 & 1 & 1 & -1 & -1 & -1 & -1 \\ 1 & 1 & -1 & -1 & 0 & 0 & 0 & 0 \\ 0 & 0 & 0 & 0 & 1 & 1 & -1 & -1 \\ 1 & -1 & 0 & 0 & 0 & 0 & 0 & 0 \\ 0 & 0 & 1 & -1 & 0 & 0 & 0 & 0 \\ 0 & 0 & 0 & 0 & 1 & -1 & 0 & 0 \\ 0 & 0 & 0 & 0 & 0 & 0 & 1 & -1 \end{pmatrix}$$

If the function $f(\zeta)$ satisfies the Lipschitz condition on the interval $[0, 1]$, then there exists a positive constant K known as the Lipschitz constant, such that for any ζ_1 and ζ_2 in the interval $[0, 1]$, the absolute difference between $f(\zeta_1)$ and $f(\zeta_2)$ is bounded by K times the absolute difference between ζ_1 and ζ_2, i.e.,

$$\left|f(\zeta_1) - f(\zeta_2)\right| \le K|\zeta_1 - \zeta_2|.$$

Consequently, the Haar approximation $f_m(\zeta)$ of the function $f(\zeta)$ takes a specific form as

$$f_m(\zeta) = \sum_{i=0}^{m-1} a_i h_i(\zeta) \quad m = 2^{q+1} \quad q = 0, 1, 2, \dots, M.$$

As shown below one can obtain the Haar wavelet's integration parameter

$$P_{i,1}(\zeta) = \int_0^{\zeta} h_i(\zeta')d\zeta'$$

$$P_{i,1}(\zeta) = \begin{cases} \zeta - \alpha & \alpha \le \zeta < \beta \\ \gamma - \zeta & \beta \le \zeta < \gamma \\ 0 & \text{elsewhere.} \end{cases}$$

The integration of $P_{i,1}(\zeta)$ becomes $P_{i,2}(\zeta) = \int_0^{\zeta} P_{i,1}(\zeta')d\zeta'$ can be written as

$$P_{i,2}(\zeta) = \begin{cases} \frac{(\zeta-\alpha)^2}{2} & \alpha \le \zeta < \beta \\ \frac{1}{4m^2} - \frac{(\gamma-\zeta)^2}{2} & \beta \le \zeta < \gamma \\ \frac{1}{4m^2} & \gamma \le \zeta < 1 \\ 0 & \text{elsewhere.} \end{cases}$$

proceeding like this the nth integration of Haar wavelets

$$P_{i,n}(\zeta) = \begin{cases} \frac{(\zeta-\alpha)^n}{n!} & \alpha \le \zeta < \beta \\ \frac{(\zeta-\alpha)^n - 2(\zeta-\beta)^n}{n!} & \beta \le \zeta < \gamma \\ \frac{(\zeta-\alpha)^n - 2(\zeta-\beta)^n + (\zeta-\gamma)^n}{n!} & \gamma \le \zeta < 1 \\ 0 & \text{elsewhere.} \end{cases}$$

A multi-resolution analysis(MRA) is the best technique to study wavelets.

A multi-resolution analysis (MRA) stands out as a powerful and comprehensive technique for studying wavelets. It provides a systematic framework to analyze wavelet functions and their properties across different scales or resolutions. MRA allows for the decomposition and reconstruction of signals or functions in a hierarchical manner, capturing their local and global characteristics. In the framework of wavelet analysis, S. Mallat and Y. Meyer [36,37] proposed the concept of MRA in 1986.

Definition 3.1. A multi-resolution analysis (MRA) is characterized by a sequence of closed subspaces, denoted as V_m, where m belongs to the set of integers. These subspaces are embedded within the space of square-integrable functions ($L^2(\mathbb{R})$) and possess the following properties [37]:

- Increasing, $V_m \subset V_{m+1},\ m \in \mathbb{Z}$.
- Density, $\cup_{m=-\infty}^{\infty}$ is dense in $L^2(\mathbb{R})$ i.e., $\overline{\cup_{m=-\infty}^{\infty} V_m} = L^2(\mathbb{R})$.
- Separation, $\cap_{j\in\mathbb{Z}} V_m = 0$.
- Scaling, $f(\zeta) \in V_m$, iff $f(2x) \in V_{m+1},\ \forall\ m \in \mathbb{Z}$.
- Orthonormality, The space V_0 contains a scaling function denoted by ϕ, which obeys the condition $\phi_{0,k}(\zeta) = \phi(\zeta - k)$ for $k \in \mathbb{Z}$. This scaling function acts as an orthonormal basis for V_0, preserving the property of orthogonality within the space.

By defining suitable projections of these functions onto these spaces, the space V_j may be utilized to approximate generic functions. Because the union of all V_0 forms a dense set within $L^2(\mathbb{R})$, implying that every function in $L^2(\mathbb{R})$ can be approximated with arbitrary precision using the projections from these subspaces.

4. Description of method for SPDDEs

To solve the singularity perturbed differential equations, we first use Taylor's series expansion to transform $y(\zeta - \delta)$ and $y(\zeta + \mu)$ and then use Haar wavelets to solve the problems. The first-order Taylor series as follows.

$$y(\zeta - \delta) = y(\zeta) - \delta \frac{dy}{d\zeta}, \tag{5}$$

$$y(\zeta + \mu) = y(\zeta) + \mu \frac{dy}{d\zeta}, \tag{6}$$

Substituting Eqs. (5) and (6) in (2) we obtained

$$\epsilon^2 \frac{d^2y}{d\zeta^2} + \{c(\zeta)\mu - b(\zeta)\delta\}\frac{dy}{d\zeta} + \{b(\zeta) + c(\zeta) + d(\zeta)\}y(\zeta) = R(\zeta), \quad \zeta \in [0, 1]. \tag{7}$$

To solve the problem, expand the highest order term as a Haar series

$$\frac{d^2y}{d\zeta^2} = \sum_{i=1}^{N} a_i h_i(\zeta). \tag{8}$$

Now integrate (8) from 0 to ζ we get

$$\frac{dy}{d\zeta} = \sum_{i=1}^{N} a_i P_{i,1}(\zeta) + \left.\frac{dy}{d\zeta}\right|_{\zeta=0}. \tag{9}$$

Again integrating (9) from 0 to ζ we obtain

$$y(\zeta) = \sum_{i=1}^{N} a_i P_{i,2}(\zeta) + \zeta \left.\frac{dy}{d\zeta}\right|_{\zeta=0} + y(0). \tag{10}$$

In order to find $\left.\frac{dy}{d\zeta}\right|_{\zeta=0}$ we have to integrate Eq. (10) from 0 to 1

$$y(1) - y(0) - \sum_{i=1}^{N} a_i C_i(\zeta) = \left.\frac{dy}{d\zeta}\right|_{\zeta=0}, \tag{11}$$

where

$$C_i(\zeta) = \int_0^1 P_{i,1}(\zeta) = \begin{cases} 0.5 & if\ i = 1 \\ \frac{1}{4m^2} & if\ i > 1, \end{cases}$$

use Eq. (11) in (9) we get

$$\frac{dy}{d\zeta} = \sum_{i=1}^{N} a_i P_{i,1}(\zeta) - \sum_{i=1}^{N} a_i C_i(\zeta) + y(1) - y(0), \tag{12}$$

and

$$y(\zeta) = \sum_{i=1}^{N} a_i P_{i,2}(\zeta) - \zeta \sum_{i=1}^{N} a_i C_i(\zeta) + \zeta(y(1) - y(0)) + y(0), \tag{13}$$

Substitute Eq. (8), (10) and (11) in (7) we get the following system of linear equations

$$\epsilon^2 \sum_{i=1}^{N} a_i H_i(\zeta) + (\eta c(\zeta) - b(\zeta)\delta)(\sum_{i=1}^{N} a_i P_{i,1}(\zeta) + y(1) - y(0) - \sum_{i=1}^{N} a_i C_i(\zeta)) +$$
$$(b(\zeta) + c(\zeta) + d(\zeta)) \sum_{i=1}^{N} a_i P_{i,2}(\zeta) + \zeta[y(1) - y(0) - \sum_{i=1}^{N} a_i C_i(\zeta)] + y(0) = R(\zeta), \quad \zeta \in [0, 1]. \tag{14}$$

Method for one parameter singularly perturbed equations

Consider the one parameter singularly perturbed equation

$$-\epsilon \frac{d^2 y}{d\zeta^2} + q(\zeta) y(\zeta) = f(\zeta), \quad \zeta \in (0, 1). \tag{15}$$

with Dirichlet BCs

$$y(0) = A, \quad y(1) = B.$$

By the Haar wavelet collocation method, we expand the highest order derivative in terms of Haar series and using the (8) and (13) in (15), we obtained

$$-\epsilon \sum_{i=1}^{N} a_i H_i(\zeta) + q(\zeta) \sum_{i=1}^{N} a_i P_{i,2}(\zeta) + y(0) + \zeta(y(1) - y(0) - \sum_{i=1}^{N} a_i C_i(\zeta)) = f(\zeta). \tag{16}$$

Using Newton's method, solve the system of linear equations to obtain coefficient $a_i's$ and put in Eq. (13) we get the approximate solutions.

5. Convergence analysis and error estimation

This section focuses on the convergence and error analysis for the proposed approach. A convergence theorem is developed, and the research includes an analysis of both maximum and absolute errors.

Make use of the asymptotic solution of the SPDDEs as

$$y(\zeta) = \sum_{i=1}^{\infty} a_i P_{i,2}(\zeta) - \zeta \sum_{i=1}^{\infty} a_i C_i(\zeta) + y(0) + \zeta(y(1) - y(0)). \tag{17}$$

The calculation of the jth level approximation involves the following

$$y_j(\zeta) = \sum_{i=1}^{N} a_i P_{i,2}(\zeta) - \zeta \sum_{i=1}^{N} a_i C_i(\zeta) + y(0) + \zeta(y(1) - y(0)). \tag{18}$$

Then the absolute error be

$$\begin{aligned} E_j &= \left| y(\zeta) - y_j(\zeta) \right| \\ &= \Big| \sum_{i=1}^{\infty} a_i P_{i,2}(\zeta) + y(0) - \Big(\sum_{i=1}^{N} a_i P_{i,1}(\zeta) + \zeta(y(1) - y(0) - \sum_{i=1}^{N} a_i C_i(\zeta)) + y(0) \Big) \Big| \\ &+ \zeta(y(1) - y(0) - \sum_{i=1}^{\infty} a_i C_i(\zeta)) \\ &= \sum_{i=1}^{\infty} \Big| a_i(P_{i,1}(\zeta) - \zeta C_i(\zeta)) - \sum_{i=1}^{N} a_i(P_{i,2}(\zeta) - \zeta C_i(\zeta)) \Big| \\ &= \sum_{i=N+1}^{\infty} \Big| a_i(P_{i,1}(\zeta) - \zeta C_i(\zeta)) \Big|, \end{aligned} \tag{19}$$

Now, we proceed to compute the error estimation as

$$\begin{aligned} \|E_j\|^2 &= \int_{-\infty}^{\infty} \sum_{i=N+1}^{\infty} \sum_{n=N+1}^{\infty} a_i a_n (P_{i,2}(\zeta) - \zeta C_i(\zeta))(P_{i,2}(\zeta) - \zeta C_i(\zeta)) \Big| \\ &= \sum_{i=N+1}^{\infty} \sum_{n=N+1}^{\infty} a_i a_n \int_{-\infty}^{\infty} \Big| (P_{i,2}(\zeta) - \zeta C_i(\zeta)) \Big|^2 \\ &= \sum_{i=N+1}^{\infty} \sum_{n=N+1}^{\infty} a_i a_n \int_{-\infty}^{\infty} |\phi(\zeta)|^2 d\zeta. \end{aligned} \tag{20}$$

After some calculations, we have

$$\|E_j\|^2 = \sum_{i=N+1}^{\infty} \sum_{n=N+1}^{\infty} a_i a_n K_{i,n}$$

and also,

$$\|E_j\|^2 \leq 2D\sqrt{K}\left(\frac{2^{-2(j+1)}}{3}\right)^2, \tag{21}$$

$D \geq y'(\zeta)$ and a_i, a_n are Haar wavelet coefficients, K is a constant, and $\phi(\zeta)$ is given as

$$\phi(\zeta) = \begin{cases} \frac{1}{2}(\zeta-\alpha)^2 - \zeta(1-\alpha)^2 & \text{for} \quad \zeta \in [\alpha, \beta) \\ \frac{1}{4m^2}(1-\zeta) - \frac{1}{2}((\gamma-\zeta)^2 - \zeta(\gamma-1)^2) & \text{for} \quad \zeta \in [\beta, \gamma) \\ \frac{1}{4m^2}(1-\zeta) & \text{for} \quad \zeta \in [\gamma, 1) \\ 0 & \text{elsewhere.} \end{cases}$$

It is evident from Eq. (21) that the error is inversely proportional to the Haar wavelet resolution j when $\|E_j\| \to 0$. The suggested composite scheme is convergent. For detailed calculation one can see [18,27,31].

Stability: To assess the stability of algorithms, it is crucial to examine the condition number, ensuring that the algebraic equations resulting from the discretization of the differential equation remain bounded [27,38]. We examining a system of linear equations such as (14) and (16) formulated using Haar wavelets $\mathcal{H}\mathcal{X} = \mathcal{B}$. We use matrix $\mathcal{H}$ to represent the associated Haar weights. The vector $\mathcal{X}$ stands for the unknown constants based on approximation, and $\mathcal{B}$ represents the known vector. The theoretical stability of the Haar wavelet method can be seen in [26,34,38]. For computational stability observation, we have

Definition 5.1 ([34,38]). Assume that a numerical approach for solving a differential equation produces a sequence of matrix equations of the form $\mathcal{H}\mathcal{X} = \mathcal{B}$. If the inverse of $\mathcal{H}$ exists and is bounded, then we say that the procedure is stable i.e.,

$$\|\mathcal{H}^{-1}\| \leq C,$$

where C is a constant.

Theorem 5.1. *Assume that the kth derivative exists and is bounded in [a,b] for any $M = 2^j, \quad j = 0, 1, 2, 3, \ldots$, if y_M and y is the Haar solution and exact solution then [27]*

$$\|y - y_M\|_\infty \leq \mathcal{O}\left(\frac{1}{M}\right)^2, \quad as \quad j \to \infty.$$

The convergence order and maximum error to observe the performance of Haar wavelet is defined as

$$C_R(M) = \log \frac{L_\infty(\frac{M}{2})L_\infty(M)}{\log(2)}.$$

The absolute error is defined as the highest value by which an estimate varies from the true value. It is impossible to determine both the actual value and the real error while doing a measurement. Maximum absolute error, however, is a measure of the highest possible difference from the actual value. The absolute error is defined as

$$L_2 = |y(\zeta) - y_M(\zeta)|.$$

and maximum absolute error

$$L_\infty = max|y(\zeta) - y_M(\zeta)|.$$

6. Numerical examples and discussion

Here, we provide numerical examples of one-parameter SPDEs and SPDDEs to demonstrate the effectiveness of the wavelet approach. The findings are summarized and compared to those of previously published approaches. In all the graphs $\zeta = x$ i.e., the x-axis represents the collocation points, and on the y-axis, we have the approximate solution. All the computations are done by using MATLABR2022a.

Example 6.1. Consider one parameter singular perturbed two-point BCs problem as:

$$-\epsilon\frac{d^2y}{d\zeta^2} + y = \zeta,$$

$$y(0) = 1, \quad y(1) = 1 + e^{(-1/\sqrt{\epsilon})}.$$

The exact solution is given as

$$y(\zeta) = e^{(-\zeta/\sqrt{\epsilon})} + \zeta.$$

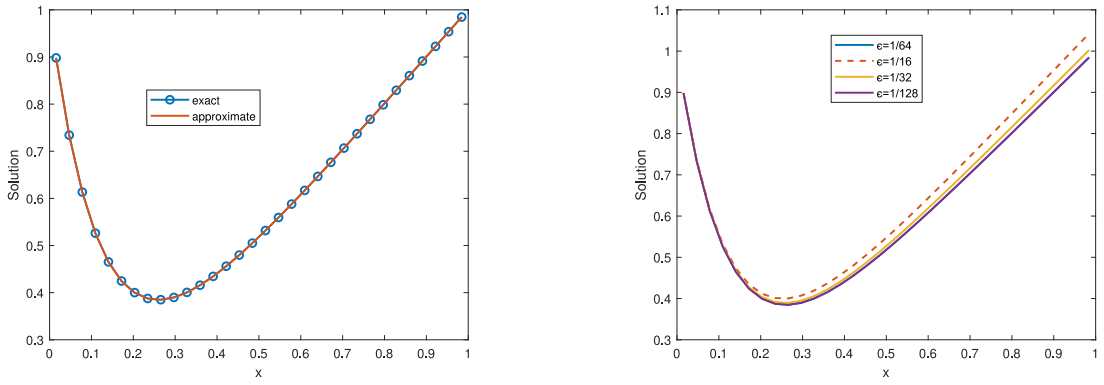

Fig. 1. (a) Approximate and exact solutions at $j = 4$ (b) Approximate solution at different values of ϵ.

Table 1
Maximum absolute error for different value ϵ and the resolution level j of Example 6.1.

ϵ	$j = 4$	$j = 6$	$j = 8$	$j = 10$
1/16	1.06e−09	5.37e−10	4.49e−12	1.55e−15
1/32	1.22e−09	4.69e−10	3.92e−12	1.22e−15
1/64	1.39e−09	3.14e−10	3.43e−12	1.33e−15
1/128	1.59e−09	2.75e−10	1.83e−12	9.99e−16
1/256	1.81e−09	8.29e−11	7.88e−13	8.88e−16
1/512	9.35e−10	5.04e−11	2.62e−13	4.44e−16
1/1024	8.16e−10	1.69e−11	1.67e−13	3.33e−16

Table 2
Comparison of maximum absolute error of Example 6.1.

ϵ	N=64 HWM	N=256 HWM	N=64 [21]	N=256[21]
1/128	1.83e−12	9.99e−16	9.81E−12	1.55E−13
1/256	7.88e−13	8.88e−16	1.05E−11	1.68E−13
1/512	2.62e−13	4.44e−16	4.19E−12	6.88E−14
1/1024	1.67e−14	3.33e−16	4.09E−13	6.88E−15

In Fig. 1(a), we present a visual comparison of the exact and approximate solutions for Example 5.1 at $\epsilon = 1/32$. Fig. 1(b) depicts the behavior of the approximate solution across different values of the perturbed parameter ϵ. For particular values of ϵ the behavior of approximate solution is depicted. By changing the values of ϵ we get the twin boundary layer. To quantify the accuracy of the approximation, we calculate the absolute errors for various values of the perturbed parameters ϵ and at different resolution levels of the Haar wavelet j. The results are compiled in Table 1. Moreover, we make a comparative analysis by contrasting HWM with an existing method [21], as presented in Table 2.

Example 6.2. Consider SPDEs as

$$-\epsilon\frac{d^2y}{d\zeta^2} + y = 1 + 2\sqrt{\epsilon}\left(e^{\left(\frac{-\zeta}{\sqrt{\epsilon}}\right)} + e^{\left(\frac{\zeta-1}{\sqrt{\epsilon}}\right)}\right),$$

$$y(0) = 1, \qquad y(1) = 0.$$

The exact solution is given as

$$y(\zeta) = 1 - (1-\zeta)\left(e^{\left(\frac{-\zeta}{\sqrt{\epsilon}}\right)} - \zeta e^{\left(\frac{\zeta-1}{\sqrt{\epsilon}}\right)}\right).$$

In Fig. 2(a), a comparison is made between the approximate and exact solutions, while Fig. 2(b) illustrates the behavior of the approximate solution for different values of the perturbed parameter ϵ. Table 3 presents the maximum absolute errors obtained through the Haar wavelet method. To provide further context, the results are compared with those from other methods, including [19,21] as presented in Table 4.

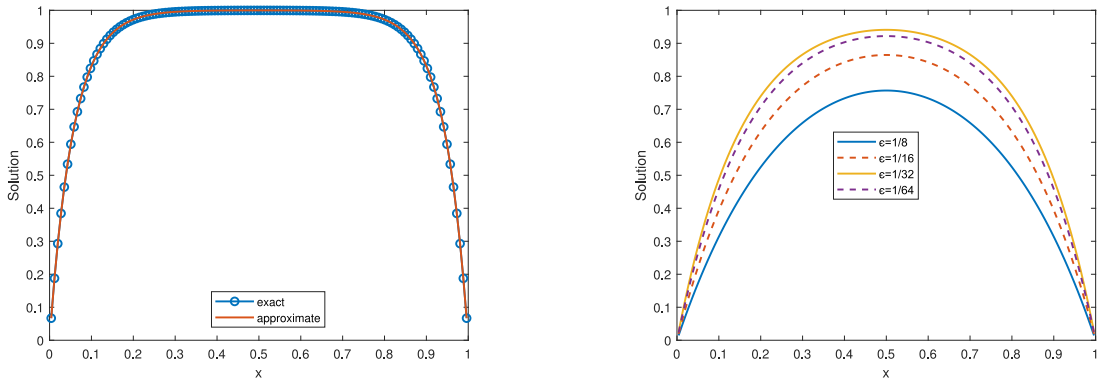

Fig. 2. (a) Approximate and exact solutions at $j = 4$ (b) Behavior of approximate solution at different value of perturbed parameter ϵ.

Table 3
Maximum absolute error for different value of ϵ and at different resolution level j of Example 6.2.

ϵ	j=4	j=6	j=8	j=10
1/16	5.09e−08	2.84e−11	1.49e−14	3.66e−15
1/32	1.42e−09	9.45e−12	2.84e−14	1.09e−15
1/64	8.80e−08	2.78e−12	8.80e−13	2.77e−15
1/128	2.86e−10	3.49e−12	2.86e−14	2.32e−15
1/256	5.88e−10	4.42e−12	3.49e−14	2.35e−16
1/512	2.35e−10	9.04e−13	1.02e−14	2.35e−16
1/1024	8.31e−11	9.38e−13	5.80e−15	2.22e−16

Table 4
Comparison of maximum absolute error.

ϵ	N=128 HWM	N=256 HWM	N=256[21]	N=256[19]
1/16	1.49e−14	6.235e- 16	7.30e−14	2.813e - 13
1/32	2.84e−14	2.810e- 16	5.22e−13	1.972e- 13
1/64	3.49e−14	2.139e- 16	3.79e−12	1.043e- 13
1/128	1.02e−14	2.67e- 15	2.68e−12	3.867e- 13
1/256	5.80e−15	1.16e- 15	2.80e−11	2.255e- 12

Table 5
Maximum absolute error for different value of ϵ and the resolution level j of Example 6.3.

ϵ	$j = 4$	$j = 6$	$j = 8$	$j = 10$
1/16	1.51e−11	3.60e−13	5.57e−14	1.55e−15
1/32	1.27e−12	2.27e−13	5.08e−14	9.99e−16
1/64	9.44e−12	2.80e−13	3.43e−14	8.88e−16
1/128	8.36e−12	1.81e−13	1.88e−14	5.55e−16
1/256	4.62e−12	1.29e−13	5.88e−15	2.22e−16
1/512	1.39e−12	5.04e−14	6.10e−15	0

Example 6.3. Consider a SPDEs as follows

$$-\epsilon \frac{d^2y}{d\zeta^2} + y = (\cos^2(\pi\zeta) + 2\epsilon\pi^2 \cos(2\pi\zeta)),$$

$$y(0) = 1, \quad y(1) = 1.$$

The exact solution is given as

$$y(\zeta) = \frac{\exp(-(1-\zeta)/\sqrt{\epsilon}) + \exp(-\zeta/\sqrt{\epsilon})}{1 + \exp(-1/\sqrt{\epsilon})} - \cos^2(\pi\zeta).$$

In Fig. 3(a), a comparison is presented between the exact and approximate solutions for Example 5.3. Fig. 3(b) showcases the behavior of the approximate solution for different values of the perturbed parameter ϵ. To provide further insight, Table 5 displays

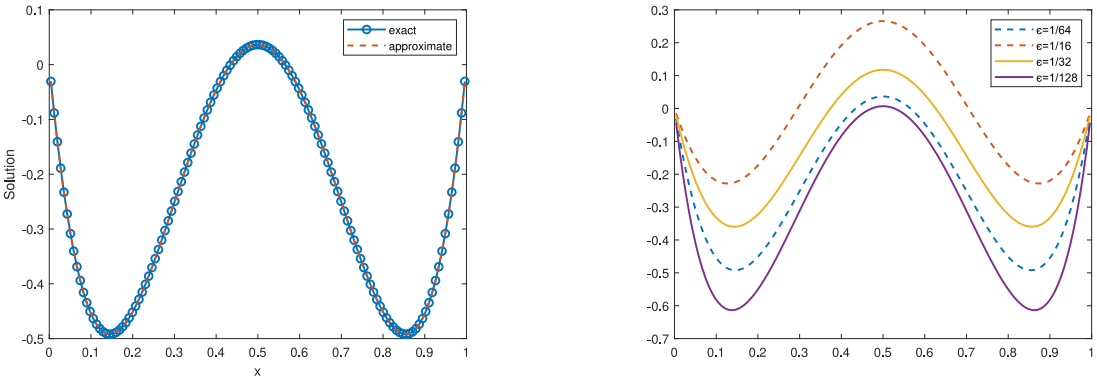

(a) (b)

Fig. 3. (a) Approximate and exact solutions at j = 4 (b) Approximate solution at different time levels.

Table 6
Comparison of maximum absolute error of ϵ of Example 6.3.

ϵ	Septic B-spline $N = 256$ [21]	Kadalbajoo and Aggarwal [25]	Exponential B-spline method [23]	HWM $N = 256$
2^{-10}	4.496e−14	5.022e−02	1.571e−03	5.08e−16
2^{-20}	3.627e−13	3.124e−02	2.815e−04	3.22e−16
2^{-25}	2.889e−12	3.124e−02	2.247e−05	1.03e−16

the maximum absolute errors for various values of the parameters ϵ. In Table 6 a comparative analysis of the results obtained from HWM with those obtained using existing methods such as [21,23,25] are presented.

Next, consider the following SPDDEs as:

Consider the SPDDEs (2) the exact solution of the two examples below having a constant coefficient is.

$$y(\zeta) = \frac{[(1-b-c-d)e^{m_2}-1]e^{m_1\zeta} - [(1-b-c-d)e^{m_1}-1]e^{m_2\zeta}}{(b+c+d)(e^{m_1}-e^{m_2})} + \frac{1}{b+c+d}. \tag{22}$$

where

$$m_1 = \frac{(b\delta - d\mu) + \sqrt{((d\mu - b\delta)^2 - 4\epsilon^2(b+c+d))}}{2\epsilon^2}.$$

$$m_2 = \frac{(b\delta - d\mu) - \sqrt{((d\mu - b\delta)^2 - 4\epsilon^2(b+c+d))}}{2\epsilon^2}.$$

Example 6.4. Consider SPDDEs with no term containing a positive shift.

$$\epsilon^2 \frac{d^2y}{d\zeta^2} - 2y(\zeta-\delta) - y(\zeta) = 1, \quad \zeta \in (0,1),$$

with BCs $y(0) = 1, -\delta \le \zeta \le 0, \quad y(1) = 1.$

The exact solution is given in (22). In Fig. 4(a), the comparison is presented between the exact and approximate solutions for Example 5.4 at $\epsilon = 0.1$ $\delta = 0.01\epsilon$. Fig. 4(b) also shows the comparison of solutions at $\epsilon = 0.01$ and $\delta = 0.03$ for resolution level $j = 6$. To provide further insight, Table 7 displays the maximum absolute errors for different values of δ and at $\epsilon = 0.1,\ 0.01$.

Example 6.5. Consider a SPDDEs as:

$$\epsilon^2 \frac{d^2y}{d\zeta^2} - 2y(\zeta) - 2y(\zeta-\mu) = 1, \quad \zeta \in (0,1),$$

with BCs $y(0) = 1, \quad y(1) = 1, \quad 1 \le \zeta \le 1+\mu.$

The exact solution is given by Eq. (22).

In Fig. 5(a), the comparison is presented between the exact and approximate solutions for Example 5.5 at $\epsilon = 0.01$ $\delta = 0.03\epsilon$. Fig. 3(b) at $\epsilon = 0.01$ and $\delta = 0.05$ at resolution level $j = 8$. Furthermore, Table 8 displays the maximum absolute errors for different values of μ and at $\epsilon = 0.1,\ 0.01$.

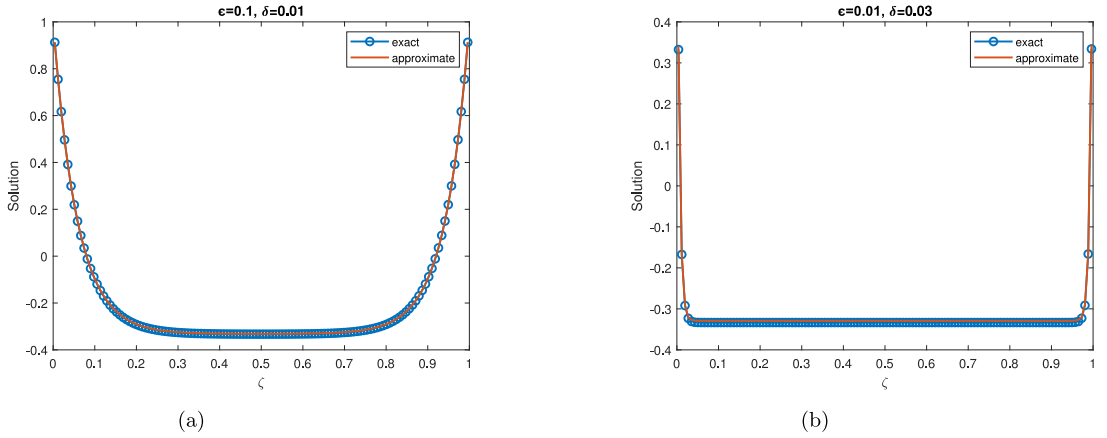

Fig. 4. (a) Approximate and exact solutions at $\epsilon = 0.1$ and $\delta = 0.01$. (b) at $\epsilon = 0.01$ and $\delta = 0.03$. with resolution $j = 6$.

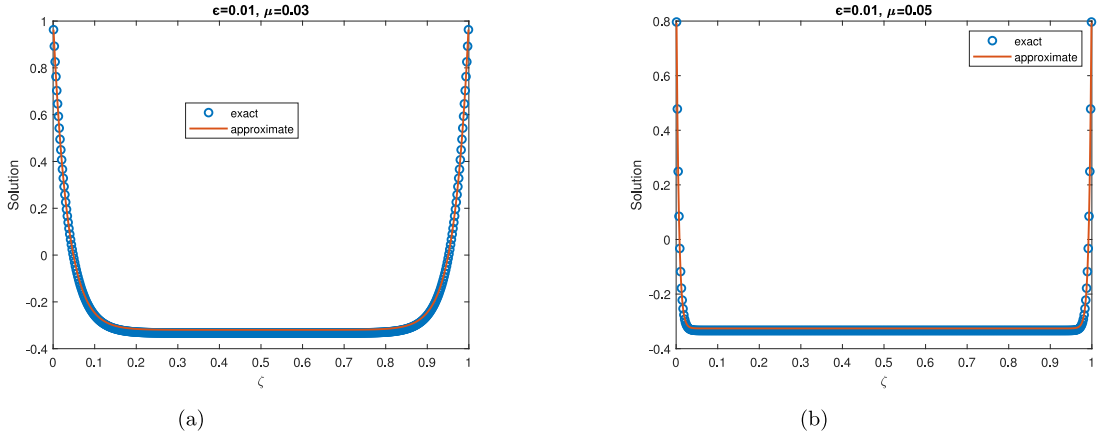

Fig. 5. (a) Comparison of approximate and exact solutions at j = 8 (b) comparison of exact and approximate solution at $\epsilon = 0.01$ and $\delta = 0.05$.

Table 7
Maximum absolute error at various level of resolution j of Example 6.4.

N	$\delta = 0.02\epsilon$	$\delta = 0.03\epsilon$	$\delta = 0.06\epsilon$	$\delta = 0.08\epsilon$
$\epsilon = 0.1$				
32	8.483e−05	3.321e−04	3.542e−04	2.632e−04
64	4.152e−05	3.277e−05	3.659e−04	2.94e−05
128	2.726e−06	1.973e−06	5.159e−05	8.742e−07
256	1.424e−07	1.005e−07	8.145e−06	1.393e−07
512	2.598e−09	3.059e−08	7.169e−08	7.596e−08
1024	1.352e−10	2.035e−09	3.152e−08	2.310e−08
$\epsilon = 0.01$				
32	7.323e−04	2.324e−04	3.432e−03	8.622e−03
64	5.112e−04	1.275e−04	1.239e−04	9.941e−04
128	2.235e−05	2.975e−06	6.235e−06	8.222e−05
256	1.564e−07	2.025e−07	7.253e−07	1.321e−07
512	6.328e−09	4.069e−08	3.256e−07	6.326e−08
1024	2.321e−09	2.145e−08	1.523e−08	9.256e−08

7. Conclusion

This study has presented the HWM as an effective approach for solving SPDDEs and one parameter SPDEs arising in the control system. The proposed method offers simplicity, computational efficiency, and accurate approximation of the solutions. Through the utilization of Taylor's series expansion and the construction of operational matrices of integration based on the Haar wavelet, the singularly perturbed problems were successfully transformed into a system of algebraic equations, which were solved using Newton's method. The applicability of the HWM is shown by means of five test problems with varying boundary conditions. In

Table 8
Maximum absolute error at various level of resolution j of Example 6.5.

N	$\mu = 0.01\epsilon$	$\mu = 0.02\epsilon$	$\mu = 0.04\epsilon$	$\mu = 0.06\epsilon$
$\epsilon = 0.1$				
32	1.661e−05	3.321e−04	2.542e−04	1.232e−04
64	1.582e−06	3.277e−05	1.659e−05	3.256e−04
128	9.853e−07	1.973e−06	5.159e−05	5.356e−06
256	1.424e−08	1.005e−07	7.145e−06	3.213e−07
512	2.598e−09	3.059e−08	4.122e−07	5.356e−08
1024	1.352e−10	2.035e−09	1.122e−08	3.210e−08
$\epsilon = 0.01$				
32	6.214e−04	2.324e−04	3.432e−03	7.152e−03
64	4.325e−04	1.215e−04	1.239e−04	6.941e−04
128	4.256e−05	3.245e−06	6.235e−06	7.222e−05
256	1.521e−07	1.025e−07	7.263e−07	1.321e−06
512	4.213e−09	5.069e−08	3.254e−07	3.326e−07
1024	2.321e−09	3.155e−08	2.524e−08	2.246e−08

addition to this, we compared our findings with the outcome of the existing methods such as Septic B-spline, cubic and exponential B-spline, and fitted operator finite difference methods [19,21,23–25]. Data shown in Tables 1 through 8 clearly emphasize that the Haar wavelet provides effective results. The graphs clearly depict that the suggested approach yields results that accord well with analytic solutions. The obtained results demonstrate that the proposed technique for solving such problems is reliable and efficient for a higher number of collocation points, and more accurate results can be obtained which is an essential feature of the method. Also, it has the potential for practical applications in a wide range of control system challenges, providing efficient numerical solutions. Further investigation and testing of this method may result in improvements in control system analysis and design.

In the future one can use the proposed technique to solve other problems such as the nonlinear and the turning point problems related to SPDDEs, singularly perturbed parabolic convection–diffusion equations, and singularly perturbed parabolic delay partial differential equations.

Declaration of competing interest

The authors declare that they have no known competing financial interests or personal relationships that could have appeared to influence the work reported in this paper.

Data availability

No data was used for the research described in the article.

Acknowledgments

The first two authors are thankful to the Central University of Haryana for providing basic facilities to carry out this research. The third author extend his appreciation to the Deanship of Scientific Research at King Khalid University for funding this work through a large group Research Project under grant number RGP2/371/44. Further, the fourth and the fifth authors appreciate Prince Sultan University for paying the APC and support through the TAS research lab.

References

[1] Mushahary P, Sahu SR, Mohapatra J. A parameter uniform numerical scheme for singularly perturbed differential-difference equations with mixed shifts. J Appl Comput Mech 2020;6(2):344–56.
[2] Ansari KJ, Amin R, Nazir H, Nawaz A, Hadi F. A computational algorithm for solving linear fractional differential equations of variable order. Filomat 2023;37(30).
[3] Khan H, Gomez-Aguilar J F, Khan A, Khan T S. Stability analysis for fractional order advection–reaction diffusion system. Physica A: Statistical Mechanics and Its Applications 521.
[4] Izadi M, Yüzbaşi Ş, Ansari Khursheed J. Application of vieta-lucas series to solve a class of multi-pantograph delay differential equations with singularity. Symmetry 2021;13:2370.
[5] Kuang Y. Delay differential equations with applications in population dynamics. Oval Road: Academic press; 1993.
[6] Lange CG, Miura RM. Singular perturbation analysis of boundary-value problems for differential-difference equations. VI. small shifts with layer behavior. SIAM J Appl Math 1994;54:249–72.
[7] Longtin A, Milton JG. Complex oscillations in the human pupil light reflex with mixed and delayed feedback. Math Biosci 1988;90:183–99.
[8] Naz H, Dumrongpokaphan T, Sitthiwirattham T, Alrabaiah H, Ansari KJ. A numerical scheme for fractional order mortgage model of economics. Results Appl Math 2023.
[9] Sahu RS, Mohapatra J. Parameter uniform numerical methods for singularly perturbed delay differential equation involving two small parameters. Int J Appl Math Comput 2019;5:1–19.
[10] Khan H, Alipour M, Khan RA, Tajadodi H, Khan A. On approximate solution of fractional order logistic equations by operational matrices of bernstein polynomials. J. Math. Comput. Sci. 2015;14:222–32.
[11] Usta F, Akyiğit M, Say F, Ansari KJ. Bernstein operator method for approximate solution of singularly perturbed Volterra integral equations. J Math Anal Appl 2022;507(2):125828.
[12] Mackey MC, Glass L. Oscillation and chaos in physiological control systems. Science 1977;197(4300):287–9.

[13] Natr L. Murray, jd: Mathematical biology. I. An introduction. Photosynthetica 2002;40:414.
[14] Hailu WS, Duressa GF. Accelerated parameter-uniform numerical method for singularly perturbed parabolic convection–diffusion problems with a large negative shift and integral boundary condition. Results Appl Math 2023;18:100364.
[15] Kevorkian J, Cole JD. Perturbation methods in applied mathematics, vol. 34. Springer Science Business Media; 2013.
[16] Duressa GF, Daba IT, Deressa CT. A systematic review on the solution methodology of singularly perturbed differential difference equations mathematics. Math 2023;11(5):1108.
[17] Raza A, Khan A, Sharma P, Ahmad K. Solution of singularly perturbed differential-difference equations and convection delayed dominated diffusion equations using Haar wavelet. Math Sci 2021;15:123–36.
[18] Raza A, Khan A. Non-uniform Haar wavelet method for solving singularly perturbed differential-difference equations of neuronal variability. Appl Appl Math Int J 2020;6:56–70.
[19] Khan A, Khandelwal P. Non-polynomial sextic spline solution of singularly perturbed boundary-value problems. Int J Comput Math 2014;5:1122–35.
[20] Kadalbajoo MK, Sharma KK. A numerical method based on finite difference for boundary value problems for singularly perturbed delay differential equation. Appl Math Comput 2008;197:692–707.
[21] Lodhi RK, Mishra HK. Septic B-spline method for second order self-adjoint singularly perturbed boundary-value problems. Ain Shams Eng J 2018;4:2153–61.
[22] Andargie A, Reddy YN. An exponentially fitted special second-order finite difference method for solving singular perturbation problems. Appl Math Comput 2007;190:1767–82.
[23] Rao S, Sekhara C, Kumar M. Exponential B-spline collocation method for self-adjoint singularly perturbed boundary value problems. Appl Numer Math 2008;10:1572–81.
[24] Khan H, Alipour M, Jafari H, Khan R A. Approximate analytical solution of a coupled system of fractional partial differential equations by bernstein polynomials. Int J Appl Comput Math 2016;2:85–96.
[25] Kadalbajoo MK, Sharma K. Numerical analysis of boundary value problems for singularly perturbed differential-difference equations, small shifts of mixed type with rapid oscillations. Commun Numer Methods Eng 2004;20:167–82.
[26] Lepik U, Hein H. Haar wavelets With applications. Math. Eng. Springer, 2014.
[27] Pandit S, Kumar M. Haar wavelet approach for the numerical solution of two parameters singularly perturbed boundary value problems. Appl Math Inf Sci 2014;8:2965–74.
[28] Sadeghi M, Vanani SK, Hafshejani JS. Numerical solution of delay differential equations using Legendre wavelet method. World Appl Sci J 2011;13:27–33.
[29] Ahmed S, Shah K, Jahan S, Abdeljawad T. An efficient method for the fractional electric circuits based on Fibonacci wavelet. Results Phys 2023;106753.
[30] Yadav P, Jahan S, Nisar KS. Fibonacci wavelet collocation method for Fredholm Integral Equations of second kind. Qual Theory Dyn Syst 2023;22:82.
[31] Ahmed S, Jahan S, Nisar KS. Hybrid Fibonacci wavelet method to solve fractional-order logistic growth model. Math Methods Appl Sci 2023;1–14.
[32] Raza A, Khan A. Haar wavelet series solution for solving neutral delay differential equations. J King Saud Univ Sci 2019;31:1070–6.
[33] Hussain B, Afroz, Jahan S. Approximate solution for proportional-delay riccati differential equations by Haar wavelet method. Poincare J Anal Appl 2021;2:155–68.
[34] Aziz I, Amin R. Numerical solution of a class of delay differential and delay partial differential equations via Haar wavelet. Appl Math Model 2016;40:10286–99.
[35] Bobisud L. Second-order linear parabolic equations with a small parameter. Arch Ration Mech Anal 1968;27(5):385–97.
[36] Daubechies I. Ten lectures on wavelets. Society for industrial and applied mathematics; 1992.
[37] Mallat SG. Multiresolution representations and wavelets. University of Pennsylvania; 1988.
[38] Ahsan M, Bohner M, Ullah A, Khan AA, Ahmad S. A Haar wavelet multi-resolution collocation method for singularly perturbed differential equations with integral boundary conditions. Math Comput Simulation 2023;204:166–80.